

# Pushing the Boundaries in CBRS Band: Robust Radar Detection within High 5G Interference

Shafi Ullah Khan\*, Michel Kulhandjian†, Debashri Roy\*

\* The University of Texas at Arlington, † Rice University

Emails: shafullah.khan@uta.edu, michel.kulhandjian@rice.edu, debashri.roy@uta.edu

**Abstract**—Spectrum sharing is a critical strategy for meeting escalating user demands via commercial wireless services, yet its effective regulation and technological enablement, particularly concerning coexistence with incumbent systems, remain significant challenges. Federal organizations have established regulatory frameworks to manage shared commercial use alongside mission-critical operations, such as military communications. This paper investigates the potential of machine learning (ML)-based approaches to enhance spectrum sharing capabilities within the Citizens Broadband Radio Service (CBRS) band, specifically focusing on the coexistence of commercial signals (e.g., 5G) and military radar systems. We demonstrate that ML techniques can potentially extend the Federal Communications Commission (FCC)-recommended signal-to-interference-plus-noise ratio (SINR) boundaries by improving radar detection and waveform identification in high-interference environments. Through rigorous evaluation using both synthetic and real-world signals, our findings indicate that proposed ML models, utilizing In-phase/Quadrature (IQ) data and spectrograms, can achieve the FCC-recommended 99% radar detection accuracy even when subjected to high interference from 5G signals up to -5dB SINR, exceeding the required limits of 20 SINR. Our experimental studies distinguish this work from the state-of-the-art by significantly extending the SINR limit for 99% radar detection accuracy from approximately 12 dB down to -5 dB. Subsequent to detection, we further apply ML to analyze and identify radar waveforms. The proposed models also demonstrate the capability to classify six distinct radar waveform types with 93% accuracy.

**Index Terms**—Radar detection, radar waveforms, 5G, CBRS, and machine learning, neural network.

## I. INTRODUCTION

**Regulations for the Shared Spectrum Usage.** The exponential growth in wireless connectivity and the emergence of data-intensive applications have significantly intensified the demand for radio spectrum [1]. To address this challenge, modern spectrum management strategies are shifting from static allocation to dynamic spectrum sharing paradigms. A prominent example is the Citizens Broadband Radio Service (CBRS) band, spanning 3.55–3.7 GHz, which was authorized by the U.S. Federal Communications Commission (FCC) to facilitate shared access among diverse users while safeguarding incumbent federal operations, primarily naval radar systems [2]. Under this framework, users are categorized into a three-tier hierarchy as shown in Fig. 1. Tier 1 for incumbents, Tier 2 for Priority Access Licensees (PAL), and Tier 3 for General Authorized Access (GAA) users [3]. Spectrum access is managed by a central entity known as Spectrum Access System (SAS) that has no control over the incumbent users, but grants access to the registered PAL and GAA users [4]. Both PAL and GAA users need to register with SAS to be considered as authorized users, and to be granted access based on their priority. The SAS relies on sensing information from an array of geographically distributed Environmental Sensing

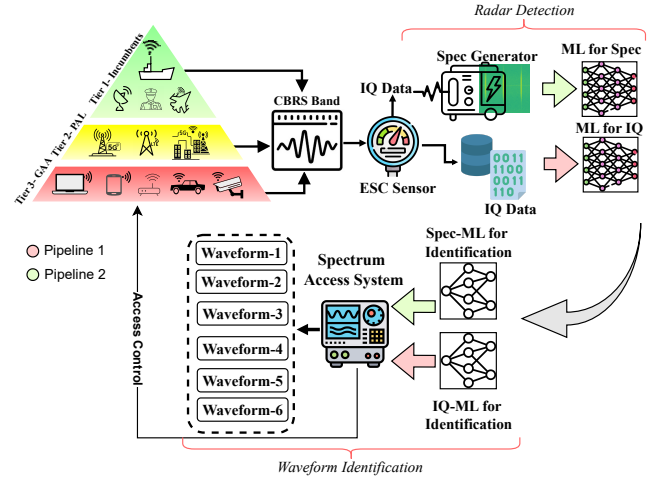


Fig. 1: Proposed machine learning pipelines for radar detection in the presence of 5G interference and subsequent radar waveform identification.

Capability (ESC) sensors for allocating the spectrum to PAL and GAA users.

While shared access improves spectral efficiency, it introduces critical challenges, particularly with regard to interference between coexisting systems. Radar signals, as primary incumbents, must be reliably detected and protected from harmful interference generated by secondary users. Hence, for a trusted shared spectrum usage, FCC has mandated that ESCs should be designed such that detection of 99% of radar pulses in signal-to-interference-plus-noise ratio (SINR) 20dB is guaranteed [5]. Commercial wireless service providers operating 4G, 5G, and private networks typically fall under the PAL and GAA categories, subject to strict transmit power constraints. Hence, with radar pulses having at least -89 dBm/MHz power, the cumulative power of additive white Gaussian noise (AWGN) and other sources of interference must be no more than -109 dBm/MHz around the ESC sensor [6].

**Pushing the Boundaries.** In this paper, we push this boundary by implementing a Machine Learning (ML)-based framework for ESC sensor that yields to 99% detection capability at SINR levels as low as -5 dB, exceeding the FCC-mandate by 25 dB. In other words, if the power of radar pulses are -94 dBm/MHz, our method will be able to provide FCC-mandated radar detection accuracy of 99% even when the noise plus interference power is as high as -89 dBm/MHz. This sets us apart from the state-of-the-art, where the ML-based approaches achieve the FCC-mandated 99% radar detection accuracy upto SINR of 20 dB [7], 17 dB [8], 16 dB [9], 15 dB [10], and

12 dB [11], hence maximum allowable noise plus interference power would be:  $-114 \text{ dBm/MHz}$ ,  $-111 \text{ dBm/MHz}$ ,  $-110 \text{ dBm/MHz}$ ,  $-109 \text{ dBm/MHz}$ ,  $-106 \text{ dBm/MHz}$ , respectively.

Additionally, our framework identifies the radar waveforms, thereby providing spectrum-access systems with precise information on the active incumbent signal and enabling more informed, interference-aware spectrum management.

**Novel Contributions.** As shown in Fig. 1, we propose two pipelines: (a) Pipeline 1 and (b) Pipeline 2. The Pipeline 1 detects the presence of radar signal and identify its waveform from the IQ data. As IQ data expose the phase information of signal, hence, prone to security vulnerabilities for sharing [12]. So, we propose Pipeline 2, which does similar radar detection and waveform identification, but from spectrograms with extra processing time for spectrogram generation time. Overall, our main contributions are summarized as follows:

- We propose a ML-based solution for detecting radar from In-phase Quadrature (IQ) data within high interference 5G signals with SINR of  $\geq -5 \text{ dB}$  (Pipeline 1).
- We further propose a ML-based solution for radar detection with SINR of  $\geq -5 \text{ dB}$  using spectrogram (Pipeline 2).
- We also propose a hierarchical classifier which does radar waveform classification, enabling fine-grained identification of radar waveforms beyond mere presence detection.
- We simulate a diverse set of radar waveforms that emulate chirp-based radar signals, generating a comprehensive dataset comprising six distinct radar waveforms with varied signal parameters.
- Finally, we validate the proposed approach using over-the-air data collected via a custom software defined radio (SDR)-based testbed in a controlled laboratory environment. The framework achieves over 99% detection accuracy on real-world signals, demonstrating strong generalization capability and compliance with regulatory standards. We release our code and data for community usage at [13].

## II. RELATED WORK

Conventional radar-sensing systems in shared-spectrum environments rely on energy detectors. Recently, there have been various ML-based efforts, such as, Lees *et al.* demonstrated the superiority of deep learning techniques over traditional radar detection algorithms by generating independent spectrograms for each 10 MHz channel and utilizing them for radar signal detection [14]. Along similar lines, Basak *et al.* trained a variant of the YOLO-lite framework to classify ten signal classes, including two Wi-Fi versions and eight drone signals in the Industrial, Scientific, and Medical (ISM) band [15]. Their study utilized over-the-air datasets containing single or multiple overlapping signals in both isolated and coexistent scenarios. Furthermore, the work in [16] employed multiple convolutional neural network (CNN) architectures for radar detection in the CBRS band, exploring both raw magnitude-based and spectrogram-based binary classification approaches to determine the presence of radar signals. Building on this direction, the ESC+ framework introduced in [8]

leveraged spectrograms and YOLO for radar detection in the CBRS band, achieving over 99% accuracy at SINR levels as high as 17 dB. Additionally, the Spec-SCAN system proposed in [10] adopted a localized scanning strategy using spectrogram analysis for confined frequency bands, reaching a recall of 99% for a single radar class at a minimum SINR of 15 dB. SenseORAN [11] embeds a modified YOLO-based xApp within the gNB's near-RT RIC to detect radar signals in the 3.5 GHz CBRS band by converting uplink IQ samples into spectrograms and maintaining a dynamic occupied-channel list; by fusing seven spectrograms per inference, it achieves 100% detection at  $\text{SINR} \geq 12 \text{ dB}$ .

**Innovation Opportunity.** While these works showcase the effectiveness of spectrogram-based deep learning approaches, to the best of our knowledge, no existing study has demonstrated robust radar detection at SINR levels lower than 12 dB. Moreover, prior literature primarily focuses on binary detection and lacks the capability to distinguish between various radar waveforms coexisting with 5G signals in the CBRS band.

## III. PROBLEM AND SOLUTION

### A. Radar Interference in 5G Wireless System

1) *Radar Specifications:* In our system, we consider a typical airborne scenario with radar transmitting an linear frequency modulated pulse (LFM) waveform. We represent the LFM waveforms by:

$$s(t) = \sum_{p=0}^{P-1} x(t - pT) \Pi\left(\frac{t - pT}{\Omega}\right), \quad (1)$$

where  $P$  is the number of pulses, and  $T$  is the pulse repetition interval,  $1/T$  pulse repetition frequency (PRF),  $\Pi(\cdot)$  is defined as a rectangular with a pulse duration/width (PW) of  $\Omega$  and the component pulse  $x(\cdot)$  is given as

$$x(t) = A e^{j(\phi_0 + 2\pi f_0 t + \pi g t^2)}, \quad (2)$$

where  $A$  is the amplitude of the pulse,  $\phi_0$  is an initial phase offset,  $f_0$  is the starting frequency, and  $g$  is the *chirp rate* defined as  $g = B/\Omega$  Hz/s, where  $B$  is the pulse bandwidth (BW).

The variation of these parameters generate different radar waveforms. We consider  $N$  type of such radar pulse waveforms:  $\mathcal{W} = \{\text{Waveform 1}, \dots, \text{Waveform } N\}$ , where  $|\mathcal{W}| = N$ .

### B. Problem Formulation

We consider a shared spectrum environment in which incumbent radar systems coexist with commercial 5G communication systems within the CBRS band. Let  $s(t)$  denote the radar signal and  $p(t)$  denote the 5G signal. The signal received at the ESC sensor is modeled as,

$$r(t) = \alpha * s(t - \tau) + \mu^{\text{CR}} * p(t) + n(t), \quad (3)$$

where ‘\*’ signify multiplication,  $\alpha$  is the backscattering coefficient of the radar echo,  $\tau$  is the propagation delay,  $\mu^{\text{CR}}$  is the interference from the transmitter, and  $n(t)$  is additive noise.

We define three signal coexistence scenarios:

- **Scenario 1 (Radar-only):**  $p(t) = 0$ . The ESC must detect radar activity and classify the waveform type.

- **Scenario 2 (5G-only):**  $s(t) = 0$ . The ESC must confirm radar absence to allow spectrum access.
- **Scenario 3 (Radar + 5G):** Both  $s(t) \neq 0$  and  $p(t) \neq 0$ . The ESC must reliably detect radar presence despite interference and further identify radar waveform from a known set. The objective is to design a decision function  $\mathcal{D}(\cdot)$  that maps received signal  $r(t)$  to a binary decision:

$$\mathcal{D}(r(t)) \in \{\text{RADAR, NO\_RADAR}\}. \quad (4)$$

In the case where  $\mathcal{D}(r(t)) = \text{RADAR}$ , a hierarchical classifier  $\mathcal{I}(\cdot)$  further identify  $N$  different radar waveforms:

$$\mathcal{I}(r(t)) \rightarrow \text{Radar Waveform} \in \mathcal{W}. \quad (5)$$

### C. Proposed Solution: Radar Detection

**Pipeline 1:** The training data matrix for IQ network is composed of the IQ samples  $\text{IQ}_{5G}$ ,  $\text{IQ}_{\text{RADAR}}$  and  $\text{IQ}_{5G+\text{RADAR}}$  from 5G, radar and overlapped RADAR+5G signals, respectively. To adapt to our binary classification problem, our radar data matrix  $X_{\text{IQ}_{\text{RADAR}}}$  consists of  $\text{IQ}_{\text{RADAR}}$  and  $\text{IQ}_{5G+\text{RADAR}}$  IQ samples and without radar data matrix  $X_{\text{IQ}_{\text{NO\_RADAR}}}$  consists of  $\text{IQ}_{5G}$  IQ samples. Overall our training data matrix is denoted as:  $X_{\text{IQ}} \in \mathbb{R}^{d_0^{\text{IQ}} \times 2} = \{X_{\text{IQ}_{\text{RADAR}}}, X_{\text{IQ}_{\text{NO\_RADAR}}}\}$ , where  $(d_0^{\text{IQ}} \times 2)$  is the dimensionality of the IQ samples with 2 representing the I and Q components. The set of the output labels are:  $\mathcal{L}_{\text{D}} = \{\text{RADAR, NO\_RADAR}\}$ . We consider the label matrix  $Y_{\text{D}} \in \{0, 1\}^{|\mathcal{L}_{\text{D}}|}$  that represent the one-hot encoding for either radar present or absent. The prediction vector  $\mathbf{s}_{\text{IQ}}^{\text{D}} \in \mathbb{R}^{|Y_{\text{D}}|}$  is generated through a Softmax activation  $\sigma$ , as:

$$\mathbf{s}_{\text{IQ}}^{\text{D}} = \sigma(f_{\theta_{\text{IQ}}^{\text{D}}}(X_{\text{IQ}})), f_{\theta_{\text{IQ}}^{\text{D}}} : \mathbb{R}^{N^{d_0^{\text{IQ}} \times 2}} \mapsto \mathbb{R}^{|Y_{\text{D}}|}. \quad (6)$$

Overall the radar detection problem is solved using the IQ network by:  $\mathcal{D}(\cdot) = \arg \max \sigma(f_{\theta_{\text{IQ}}^{\text{D}}}(\cdot))$ .

**Pipeline 2:** In this case, the spectrogram samples are denoted as:  $\mathbf{s}_{\text{RADAR}}$ ,  $\mathbf{s}_{5G}$  and  $\mathbf{s}_{\text{RADAR+5G}}$  from spectrograms of radar, 5G, and overlapped RADAR+5G signals, respectively. This data matrix is denoted as:  $X_{\text{S}} \in \mathbb{R}^{d_0^{\text{S}} \times d_1^{\text{S}} \times 3} = \{X_{\text{S}_{\text{RADAR}}}, X_{\text{S}_{\text{NO\_RADAR}}}\}$ , with  $X_{\text{S}_{\text{RADAR}}}$  consisting of  $\mathbf{s}_{\text{RADAR}}$  and  $\mathbf{s}_{\text{NO\_RADAR}}$  spectrogram samples and  $X_{\text{S}_{\text{NO\_RADAR}}}$  consisting of  $\mathbf{s}_{5G}$  samples. The  $(d_0^{\text{S}} \times d_1^{\text{S}} \times 3)$  gives the dimensionality of spectrogram images with 3 representing the three channels for RGB. The labels and label matrix are same as IQ network. The prediction vector  $\mathbf{s}_{\text{S}}^{\text{D}} \in \mathbb{R}^{|Y_{\text{D}}|}$  through a Softmax activation  $\sigma$ , is denoted as:

$$\mathbf{s}_{\text{S}}^{\text{D}} = \sigma(f_{\theta_{\text{S}}^{\text{D}}}(X_{\text{S}})), f_{\theta_{\text{S}}^{\text{D}}} : \mathbb{R}^{N^{d_0^{\text{S}} \times d_1^{\text{S}} \times 3}} \mapsto \mathbb{R}^{|Y_{\text{D}}|} \quad (7)$$

In this case,  $\mathcal{D}(\cdot) = \arg \max \sigma(f_{\theta_{\text{S}}^{\text{D}}}(\cdot))$ .

### D. Proposed Solution: Radar Waveform Identification

After radar is detected within a signal, we propose the second stage of hierarchical classifier to detect the waveform of the radar signal out of  $N$  possibilities.

**Pipeline 1:** In this case, the data matrix consists of IQ samples with radar signals, hence  $X_{\text{IQ}_{\text{RADAR}}} \in \mathbb{R}^{d_0^{\text{IQ}} \times 2}$ . The label matrix is  $Y_{\text{I}} \in \{0, 1\}^N$  in the one-hot encoding representation to signify  $N$  possibilities of radar waveforms. The prediction vector  $\mathbf{s}_{\text{IQ}}^{\text{I}} \in \mathbb{R}^{|Y_{\text{I}}|}$  through a Softmax activation  $\sigma$ , is denoted as:

$$\mathbf{s}_{\text{IQ}}^{\text{I}} = \sigma(f_{\theta_{\text{IQ}}^{\text{I}}}(X_{\text{IQ}_{\text{RADAR}}})), f_{\theta_{\text{IQ}}^{\text{I}}} : \mathbb{R}^{N^{d_0^{\text{IQ}} \times 2}} \mapsto \mathbb{R}^{|Y_{\text{I}}|} \quad (8)$$

We use IQ Network as:  $\mathcal{I}(\cdot) = \arg \max \sigma(f_{\theta_{\text{IQ}}^{\text{I}}}(\cdot))$ . to solve the radar waveform identification problem.

**Pipeline 2:** Similar to the Pipeline 1, the data matrix and label matrices are:  $X_{\text{S}_{\text{RADAR}}} \in \mathbb{R}^{d_0^{\text{S}} \times d_1^{\text{S}} \times 3}$  and  $Y_{\text{I}} \in \{0, 1\}^N$ , respectively. The prediction vector  $\mathbf{s}_{\text{S}}^{\text{I}} \in \mathbb{R}^{|Y_{\text{I}}|}$  is:

$$\mathbf{s}_{\text{S}}^{\text{I}} = \sigma(f_{\theta_{\text{S}}^{\text{I}}}(X_{\text{S}_{\text{RADAR}}})), f_{\theta_{\text{S}}^{\text{I}}} : \mathbb{R}^{N^{d_0^{\text{S}} \times 2}} \mapsto \mathbb{R}^{|Y_{\text{I}}|} \quad (9)$$

In this case,  $\mathcal{I}(\cdot) = \arg \max \sigma(f_{\theta_{\text{S}}^{\text{I}}}(\cdot))$ .

## IV. EXPERIMENTS

To validate our proposed pipelines for both radar detection and waveform identification, we generate synthetic dataset with varies SINR and real-world dataset from a SDR testbed.

### A. Synthetic Dataset

We generate a synthetic IQ dataset using MATLAB's Communication, Array Processing, and 5G Toolboxes. The simulation involves creating a 5G physical layer signal by placing a base station, multiple user equipments, and a radar system at specific 3D locations. The dataset features a radar signal with different SINRs relative to 5G and noise levels, sampled at 61.44 MHz with a center frequency of 3.6 GHz, modeling the interaction between radar and 5G signals in a realistic shared spectrum environment. We define SINR as  $10 \times \log_{10}(P_{\text{radar}}/P_{\text{noise}})$ , where  $P_{\text{radar}}$  is peak radar power per MHz, and  $P_{\text{noise}}$  is average noise plus interference power per MHz of the radar band. We vary the power of radar pulses in the range of  $-89$  to  $-79$  dBm/MHz to emulate SINRs in the range of  $-20$  to  $20$  dB, with  $5$  dB interval. For the noise and interference power, we go upto  $25$  dB beyond FCC limit, and allow the noise and interference power to vary in the range of  $-109$  to  $-84$  dBm/MHz. Overall, our synthetic dataset contains  $\sim 13608$  generated signals from three categories: (a) radar pulses only, (b) 5G signals only, and (c) radar pulses overlapped with 5G signals, out of which we utilize 4536 samples with SINR varying between  $-5$  dB to  $5$  dB for this work. We consider six distinct LFM chirp waveforms, representative of common radar types used in tactical and military communications. Table I, shows a wide range of radar system characteristics. BIN1-A and BIN1-B represent short-duration, high-PRF radars, that are suitable for high-resolution target tracking or missile guidance systems. Their high chirp rates (up to  $4$  GHz/s) make them ideal for fine range discrimination. BIN2 and BIN3 waveforms correspond to medium- and long-pulse systems, often used in surveillance, marine, or ground-based tracking radars.

TABLE I: Specifications of various radar waveforms.

Waveform	PW (μs)	PRF (Hz)	BW (MHz)	Chirp Rate (GHz/s)
BIN1-A	1	20,000	1	1000
BIN1-B	2	30,000	8	4000
BIN2-A	50	200	20	400
BIN2-B	100	200	30	300
BIN3-A	10	100	5	500
BIN3-B	50	150	15	300

### B. Real-world Dataset

Our SDR testbed consists of multiple USRP B210 devices in a controlled laboratory environment. Specifically, one USRP B210 is configured to transmit radar pulses, another to transmit 5G waveforms, and a third to function as a receiver, capturing the over-the-air signals. The experiment incorporates six distinct radar pulse types alongside 5G

signals, transmitted under various controlled conditions. To evaluate the robustness of the framework under noisy and dynamic channel conditions, we systematically varied the distance between the transmitters and the receiver, thereby introducing controlled noise levels into the received signal. Multiple samples were collected for each configuration to ensure statistical validity. Additionally, signal diversity was introduced by varying the transmission bandwidth of the 5G waveforms. All transmissions are carried out at a center frequency of 3.65 GHz with a constant sampling rate of 50 MS/s and a fixed antenna gain of 85 dB. The experimental setup is illustrated in Fig. 2, while the detailed parameter configurations and signal characteristics are summarized in Table II.

TABLE II: The specification of various real world data collection scenario. We emulate various signal interference by varying the distance of the radar transmitter and 5G transmitter from the receiver.

Signal Type	Distance (Tx-Rx)	BW (MHz)	Samp Rate	Center Freq (GHz)	Samples	Ant Gain
Radar	1-8 ft	20	50 MS/s	3.65	420	85 dB
5G	1-8 ft	5-50	50 MS/s	3.65	480	85 dB
Radar + 5G	1-8 ft	20 + 5-50	50 MS/s	3.65	480	85 dB

**Dataset Availability:** Overall, the statistics of the IQ and spectrogram data are: (a) 1,512 for each SINR  $-5 \text{ dB}$ ,  $0 \text{ dB}$ ,  $5 \text{ dB}$  and (b) 918 samples for real-world data, incurring total number of 5,454. Samples of the spectrograms and IQ data of both the synthetic and real datasets are available at [13].

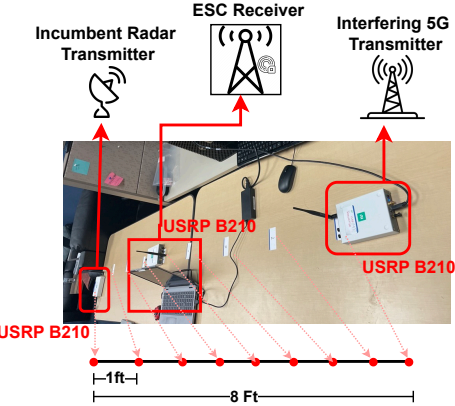


Fig. 2: Laboratory testbed emulating a real-world spectrum-coexistence scenario with an incumbent radar transmitter, ESC receiver, and interfering 5G transmitter.

### C. Neural Network (NN) Architectures

The details of NN models  $f_{\theta_0^D}^{IQ}(\cdot)$  and  $f_{\theta_0^S}^S(\cdot)$  (discussed in Section III-C) for the *radar detection* part of the hierarchical classifier are shown in Fig. 3 (a) and (b). Similarly, the NN models  $f_{\theta_1^D}^{IQ}(\cdot)$  and  $f_{\theta_1^S}^S(\cdot)$  (as discussed in Section III-D) for the *radar waveform identification* part of the hierarchical classifier is shown in Fig. 3 (a) and (c). We exploit categorical cross-entropy loss for training using Tensorflow backend with 70/20/10 train/val/test ratio, details of other parameters for different NN model are in Table III.

**Evaluation Metrics.** We use standard classification metrics: accuracy, precision, recall, F1 score, and inference time to

TABLE III: Hyperparameter settings for training various NN models.

Hyperparameter	ViT (Fig. 3 (b))	CNN (Fig. 3 (c))	ANN (Fig. 3 (a))
Batch size	32	32	16
Input channels	RGB (3)	RGB (3)	–
Learning rate	$5 \times 10^{-4}$	$5 \times 10^{-4}$	$1 \times 10^{-4}$
Activation	Softmax	Softmax	Softmax
Loss	categorical crossentropy	categorical crossentropy	categorical crossentropy
Epochs	200	100	100
Optimizer	Adam	Adam	Adam
Test split	15%	15%	30%
Validation split	10%	10%	10%
Dropout rate	0.1	–	–
Projection dimension & layers	64 (4 transformer layers)	–	–
Kernel size	16	$3 \times 3$	–
Number of Conv layers	1	4	–

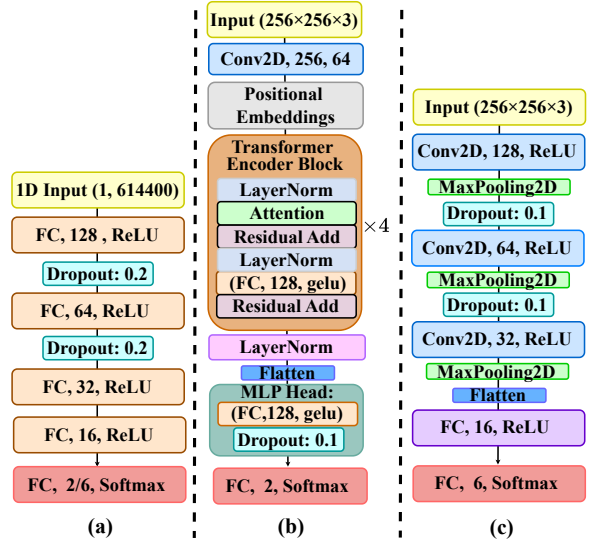


Fig. 3: Different neural network architectures used for the two parts of hierarchical classifier using: (a) IQ samples for radar detection (Pipeline 1) and waveform identification (Pipeline 2), (b) Spectrograms for radar detection (Pipeline 2), (c) Spectrograms for radar waveform identification (Pipeline 2).

validate our proposed pipelines for both radar detection and radar waveform identification task.

### D. Experimental Results on Radar Detection

In the first set of experiments, we evaluate the *radar detection* part of the hierarchical classifier that detects radar presence. The performance of all the pipelines across different datasets is shown in Table IV. Overall, Pipeline 2 gives better performance than Pipeline 1. Hence, we perform a trade-off analysis of these two pipelines in terms of inference time for radar detection and performance.

**Observation 1.** We observe that the spectrogram-based Pipeline 2 maintain  $\geq 99\%$  accuracy even at  $-5 \text{ dB}$  SINR, while the IQ-based Pipeline 1 fails to achieve FCC mandated 99% radar detection accuracy (refer to Table IV).

**Trade-off Analysis of Pipeline 1 vs. Pipeline 2.** Fig. 4 illustrates the inference time radar detection vs. accuracy trade-off between the spectrogram-based Pipeline 2 and IQ-based Pipeline 1. The Pipeline 2 applies

TABLE IV: Performance of Pipeline 1 and 2 for radar detection.

Signal	Metrics (%)	Spectrograms	IQ Samples
		Pipeline 2	Pipeline 1
SINR 5 dB	Overall Accuracy	99.8	98.02
	Radar Precision	99.6	100
	False Positives	0	0
	Recall	99.5	94.17
SINR 0 dB	Overall Accuracy	99.7	97.64
	Radar Precision	99.6	99.5
	False Positives	0	0
	Recall	99.5	93.27
SINR -5 dB	Overall Accuracy	99.5	96.54
	Radar Precision	99.5	98.25
	False Positives	0	0
	Recall	99.5	91.17
Real Data	Overall Accuracy	99.5	91.10
	Radar Precision	99.6	97.40
	False Positives	0	0
	Recall	99.5	88.20

a Short-time Fourier Transform (STFT) to the 20 ms of IQ values sampled at 61.44 MHz, incurring approximately 80 ms to generate the time–frequency spectrogram followed by 33 ms for model inference (total 113 ms). Whereas the Pipeline 1 completes end-to-end inference in 37 ms. Despite the additional 76 ms preprocessing overhead, the Pipeline 2 achieves 99.95% accuracy, which is 8% higher than that of the Pipeline 1’s 92.89%, by leveraging detailed time–frequency features that bolster robustness under severe interference.

**Observation 2.** *We observed that despite an approximately threefold increase in end-to-end inference latency (113 ms vs. 37 ms), the spectrogram-based model delivers an 8% higher accuracy (99.95 % vs. 92.89 %), highlighting the latency–accuracy trade-off inherent in time–frequency processing (refer Fig. 4).*

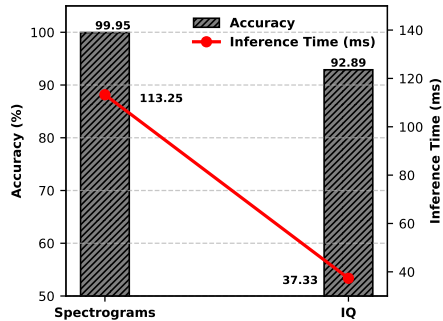


Fig. 4: Trade-off between the inference time and the radar detection accuracy at SINR= -5dB.

**t-SNE-Based Feature Space Visualization for Pipeline 1 vs. Pipeline 2.** t-distributed stochastic neighbor embedding (t-SNE) is a nonlinear dimensionality reduction technique used to visualize high-dimensional data in low-dimensional space while preserving local structure [17]. Figure 5 illustrates the 3D t-SNE projections of the learned feature spaces from the NN models of both the pipelines. As shown in Fig. 5a, the NN model of Pipeline 1 produces less distinct clusters, with noticeable overlap between the RADAR and NO\_RADAR classes. This suggests that raw IQ inputs lack sufficient discriminative characteristics needed for precise classification in congested spectral environments.

Conversely, the NN model of Pipeline 2 in Fig. 5b achieves well-separated clusters for all three classes, indicating superior representational capability. The richer time–frequency structure captured in spectrograms allows the NN model to extract more salient features, enabling enhanced class separability.

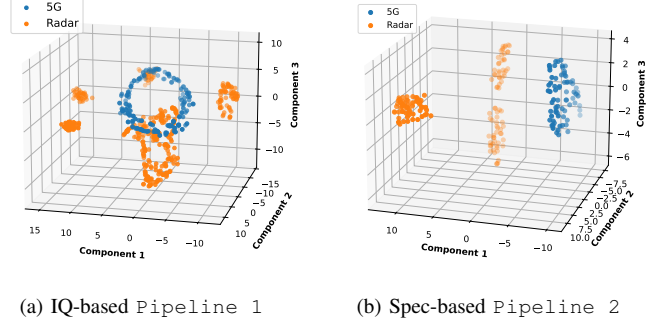


Fig. 5: Comparison of feature separability via 3D t-SNE for IQ-based Pipeline 1 and spectrogram-based Pipeline 2. Spectrogram features exhibit better class distinction.

**Comparison with state-of-the-art.** Table V presents a comparative analysis between the proposed framework and several state-of-the-art radar detection methods developed for the CBRS band. While existing approaches such as RadYOLOLet [9], Waldo [8], DeepRadar [7], Spec-SCAN [10] and SenseORAN [11] achieve high detection accuracy, they are primarily constrained to operating at SINR levels no lower than 12 dB. In contrast, our method achieves 100% recall even in harsh interference environments, operating reliably at an SINR as low as -5 dB, thus significantly surpassing the SINR tolerance of previous work.

In addition to robust detection, the proposed framework also performs fine-grained radar waveform classification, identifying six distinct types of radar. This level of granularity exceeds that of DeepRadar and RadYOLOLet, which classify up to five radar types, while Waldo, Spec-SCAN and SenseORAN only considered one type of identification. The combined ability to detect radar at lower SINR levels and identify more radar types highlights the enhanced sensitivity and utility of our system for spectrum co-existence and dynamic spectrum access enforcement.

**Observation 3.** *We observe that our framework extends reliable detection down to -5 dB SINR while classifying six distinct radar waveforms, surpassing prior CBRS detectors in both interference robustness and identification granularity (See Table V).*

TABLE V: Comparison of state-of-the-art radar detection methods vs. proposed approach (Pipeline 2).

Paper	SINR	Recall	Radar Identification
RadYOLOLet [9]	$\geq 16$ dB	100%	5 Types
Waldo [8]	$\geq 17$ dB	100%	1 Type
DeepRadar [7]	$\geq 20$ dB	99%	5 Types
Spec-SCAN [10]	$\geq 15$ dB	100%	1 Type
senseORAN [11]	$\geq 12$ dB	100%	1 Type
<b>Ours (Pipeline 2)</b>	$\geq -5$ dB	99.5%	<b>6 Types</b>

#### E. Experimental Results on Radar Waveform Identification

Figure 6 illustrates the comparative performance of spectrogram-based Pipeline 2 and IQ-based Pipeline

1 in terms of accuracy and F1-score across varying SINR levels and real testbed data. It is evident that Pipeline 2 maintain consistently high performance across all conditions, including severe interference at  $SINR = -5$  dB and real-world measurements. This resilience can be attributed to the time-frequency representation provided by spectrograms, which enables the model to capture both transient and stationary signal features essential for distinguishing radar signal characteristics. Notably, the spectrogram model achieves approximately 78% accuracy on real data and exceeds 99% in accuracy, indicating strong discriminability even under domain shift and practical noise. Conversely, IO-based models

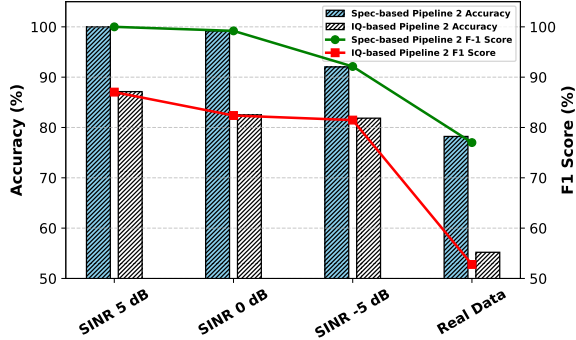


Fig. 6: Performance comparison of Pipeline 1 and Pipeline 2 for radar waveform identification.

exhibit a steeper decline in both accuracy and F1-score, especially at lower SINR values and under real-world conditions. This degradation highlights the limitations of using raw in-phase and quadrature components, which lack explicit temporal and spectral structure and thus fail to expose the discriminative properties required for robust radar signal classification. Specifically, in radar parameter identification tasks involving pulse width, chirp bandwidth, and PRF variations, the absence of structured feature representations in IQ data results in lower model confidence and generalization. This reinforces the necessity of time-frequency domain representations in spectrum sensing applications involving heterogeneous radar signals.

**Observation 4.** We observed that Pipeline 2 maintain  $> 99\%$  accuracy for synthetic data with  $SINR \geq 0$  dB, while Pipeline 1 reaches maximum accuracy of 88% for radar waveform identification for synthetic data with  $SINR = 5$  dB (see Fig. 6).

## V. CONCLUSIONS

In this work, we propose a robust ML-based pipeline for radar detection and waveform identification within the CBRS band. Unlike traditional energy detection methods that degrade under low SINR conditions, our approach leverages high-resolution spectrogram representations to effectively detect radar signals even at SINR levels as low as  $-5$  dB, significantly exceeding the FCC-mandated threshold of 99% detection accuracy threshold set at 20 dB. This enables the commercial 5G users to transmit at high as  $-84$  dBm/MHz when the co-existing radar power is  $-94$  dBm/MHz and still able to detect radar presence with 99% accuracy. Furthermore, the framework extends beyond detection of radar by incorporating fine-grained identification of six types of radar waveforms, allowing more context-aware spectrum management. The proposed ML-based pipelines are validated on

diverse datasets to demonstrate improvement over state-of-the-art methods. Future scopes include the radar parameter estimation and distributed execution of the proposed pipelines. The authors have provided public access to their code and data at [13].

## ACKNOWLEDGMENT

The authors gracefully acknowledge the sponsorship of the SDR devices from Dr. Stephen Hary through the Airforce Research Lab SDR Challenge program and funding from the US National Science Foundation (CNS 2526490).

## REFERENCES

- [1] S. A. A. Shah, E. Ahmed, M. Imran, and S. Zeadally, “5g for vehicular communications,” *IEEE Communications Magazine*, vol. 56, no. 1, pp. 111–117, 2018.
- [2] Federal Communications Commission, “3.5 GHz Band Overview,” <https://www.fcc.gov/wireless/bureau-divisions/mobility-division/35-ghz-band/35-ghz-band-overview>, 2025, accessed: 27 May 2025.
- [3] S. U. Khan, M. Kulhandjian, and D. Roy, “In-Network Fusion for High Interference Signal Detection within CBRS Band,” in *IEEE International Conference on Computer Communications (INFOCOM)*, May 2025, [Accepted].
- [4] “FCC Releases Rules for Innovative Spectrum Sharing in 3.5 GHz Band,” <https://docs.fcc.gov/public/attachments/FCC-15-47A1.pdf>, accessed: May 2022.
- [5] F. H. Sanders, J. E. Carroll, G. A. Sanders, R. L. Sole, J. S. Devereux, and E. F. Drocetta, “Procedures for laboratory testing of environmental sensing capability sensor devices,” *National Telecommunications and Information Administration, Technical Memorandum TM*, pp. 18–527, 2017.
- [6] “Requirements for Commercial Operation in the U.S. 3550-3700 MHz Citizens Broadband Radio Service Band,” <https://winnf.memberclicks.net/assets/CBRS/WINNF-TS-0112.pdf>, accessed: May 2022.
- [7] S. Sarkar, M. Buddhikot, A. Baset, and S. K. Kaser, “Deepradar: a deep-learning-based environmental sensing capability sensor design for cbrs,” in *Proceedings of the 27th Annual International Conference on Mobile Computing and Networking*. New York, NY, USA: Association for Computing Machinery, 2021, p. 56–68. [Online]. Available: <https://doi.org/10.1145/3447993.3448632>
- [8] N. Soltani, V. Chaudhary, D. Roy, and K. Chowdhury, “Finding waldo in the cbrs band: Signal detection and localization in the 3.5 ghz spectrum,” in *GLOBECOM 2022 - 2022 IEEE Global Communications Conference*, 2022, pp. 4570–4575.
- [9] S. Sarkar, D. Guo, and D. Cabric, “Radyololet: Radar detection and parameter estimation using yolo and wavelet,” *IEEE Transactions on Cognitive Communications and Networking*, pp. 1–1, 2024.
- [10] R. Hazari, G. Singh, D. Renjith, D. Krishnan, P. B. H. Olufowobi, and D. Roy, “Spec-scan: Spectrum learning in shared channel using neural networks,” in *2025 IEEE 22nd Consumer Communications & Networking Conference (CCNC)*, 2025, pp. 1–6.
- [11] G. Reus-Muns, P. S. Upadhyaya, U. Demir, N. Stephenson, N. Soltani, V. K. Shah, and K. R. Chowdhury, “Senseoran: O-ran-based radar detection in the cbrs band,” *IEEE Journal on Selected Areas in Communications*, vol. 42, no. 2, pp. 326–338, 2024.
- [12] A. U. Haq, S. S. Sefati, S. J. Nawaz, A. Mihovska, and M. J. Beliatis, “Need of uavs and physical layer security in next-generation non-terrestrial wireless networks: Potential challenges and open issues,” *IEEE Open Journal of Vehicular Technology*, vol. 6, pp. 554–595, 2025.
- [13] TWIST-Lab, “Radar-detection-pushing-bound,” <https://github.com/TWIST-Lab/Radar-detection-pushing-bound>, 2025, GitHub repository. Accessed: May 29, 2025.
- [14] W. M. Lees, A. Wunderlich, P. J. Jeavons, P. D. Hale, and M. R. Souri, “Deep learning classification of 3.5-ghz band spectrograms with applications to spectrum sensing,” *IEEE Transactions on Cognitive Communications and Networking*, vol. 5, no. 2, p. 224–236, Jun. 2019. [Online]. Available: <http://dx.doi.org/10.1109/TCNN.2019.2899871>
- [15] S. Basak, S. Rajendran, S. Pollin, and B. Scheers, “Combined rf-based drone detection and classification,” *IEEE Transactions on Cognitive Communications and Networking*, vol. 8, no. 1, pp. 111–120, 2022.
- [16] R. Caromi, A. Lackpour, K. Kallas, T. Nguyen, and M. Souri, “Deep learning for radar signal detection in the 3.5 ghz cbrs band,” in *2021 IEEE International Symposium on Dynamic Spectrum Access Networks (DySPAN)*, 2021, pp. 1–8.
- [17] W. Zaman, M. F. Siddique, S. U. Khan, and J.-M. Kim, “A new dual-input cnn for multimodal fault classification using acoustic emission and vibration signals,” *Engineering Failure Analysis*, p. 109787, 2025.